IEEE Photonics Journal
An IEEE Photonics Society Publication

Open Access

Performance Analysis of Single-Photon Avalanche Diode Underwater VLC System Using ARQ

Volume 9, Number 5, October 2017

Taniya Shafique
Osama Amin
Mohamed Abdallah
Imran Shafique Ansari
Mohamed-Slim Alouini
Khalid Qaraqe

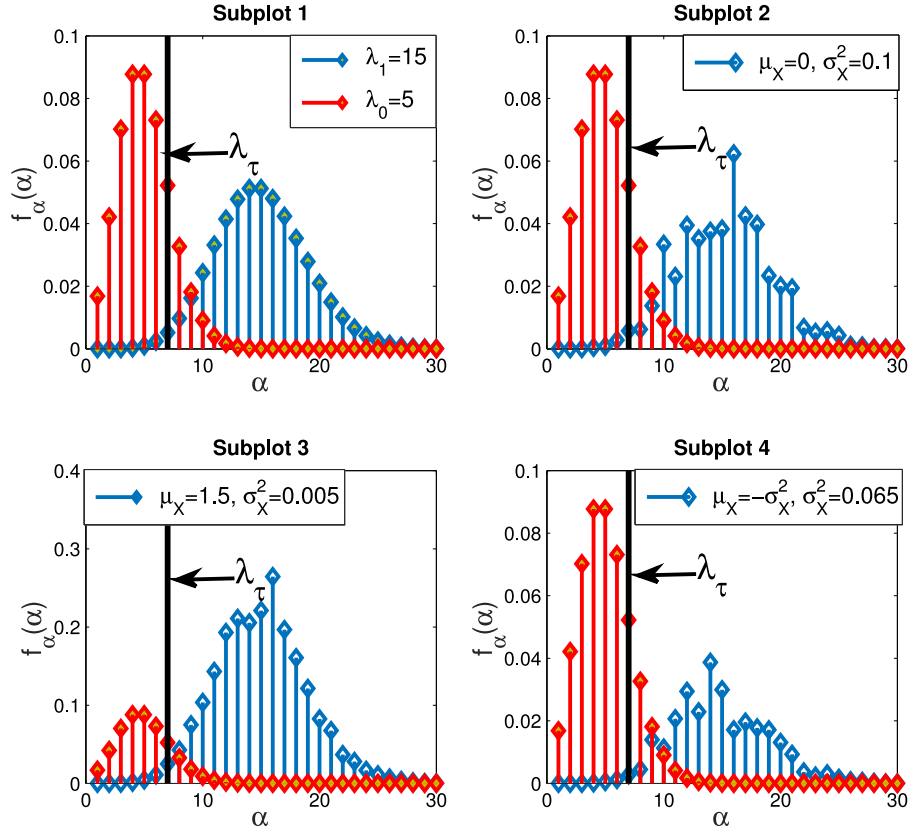

DOI: 10.1109/JPHOT.2017.2743007
1943-0655 © 2017 IEEE

Performance Analysis of Single-Photon Avalanche Diode Underwater VLC System Using ARQ

Taniya Shafique,[1] Osama Amin,[2] Mohamed Abdallah,[3] Imran Shafique Ansari,[1] Mohamed-Slim Alouini,[2] and Khalid Qaraqe[1]

[1]Electrical and Computer Engineering, Texas A&M University at Qatar, Doha 34110, Qatar
[2]Computer, Electrical and Mathematical Science and Engineering Division (CEMSE), King Abdullah University of Science and Technology (KAUST), Thuwal 23955-6900, Saudi Arabia
[3]College of Science and Engineering, Hamad Bin Khalifah University (HBKU), Doha, Qatar

DOI:10.1109/JPHOT.2017.2743007

Manuscript received August 1, 2017; revised August 16, 2017; accepted August 17, 2017. Date of publication August 22, 2017; date of current version September 8, 2017. This work was supported by the NPRP award [NPRP 8 -648-2-273] from the Qatar National Research Fund (a member of the Qatar Foundation). The statements made herein are solely the responsibility of the author(s). Corresponding author: Mohamed Abdallah (e-mail: moabdallah@hbku.edu.qa).

Abstract: Single-photon avalanche diode (SPAD) has recently been introduced as a powerful detector for long-distance underwater visible light communication (UVLC). In this paper, the performance of the SPAD detector in UVLC is analyzed considering the effect of the turbulence-induced fading resulting from air bubbles in addition to the combined effect of attenuation and scattering. An automatic repeat request (ARQ) system is adopted to mitigate different underwater impairments and reduce the error probability at the receiver side. Approximate packet error rate (PER) expressions are derived using Laguerre Gauss polynomial for a finite number of transmission. Next, the average energy efficiency and throughput are analyzed to account for the increased energy consumption cost and the decreased effective transmission rate, which results from adopting the ARQ scheme. Finally, different numerical results are introduced to verify the derived PER expressions, demonstrate the ability of the proposed ARQ system in extending the transmission range, and show the tradeoff between energy efficiency and throughput.

Index Terms: Underwater visible light communication (UVLC), optical wireless communications, single-photon avalanche diode (SPAD), automatic repeat request (ARQ), error probability, throughput, energy efficiency.

1. Introduction

Developing robust and efficient underwater communication links has drawn great attention to support different applications in scientific, military and industrial fields. Unlike traditional terrestrial radio communications, the underwater communication faces distinct environmental challenges such as water turbidity, temperature variation, salt concentration, waves and bubbles. To this end, different underwater communication technologies have been introduced to exchange data for different communication ranges. Radio frequency technology can support high data rates for few meters where the electromagnetic waves are heavily affected by propagation loss. On the other hand, acoustic technology has a very limited data rate but can support large distances [1]. Two-way underwater

acoustic systems are realized by continuous automatic repeat and request (ARQ) protocol using half-duplex communications. The continuous ARQ protocol is used instead of stop-and-wait ARQ to compensate the long propagation delay of the underwater acoustic system [2]. Both the acoustics and the radio frequency technologies lack the tendency to meet the demands of future underwater wireless communications such as high data rates for long distances. To support higher data rates than the aforementioned technologies, optical wireless communication has been introduced as a possible candidate for underwater communications [3].

Optical wireless communication is carried out through a 400 THz band that includes infrared, visible and ultraviolet sub-bands. Visible light communication has many promising practical applications that make use of the existing infrastructure while meeting the illumination constraints such as indoor high-speed communication and localization [4]–[6]. Moreover, visible light communication is adopted for underwater communications due to the wavelength sensitivity of light propagation, where the green/blue wavelength (450 nm–520 nm) offers the least attenuation [7]. Underwater visible light communication (UVLC) can be used in different environmental applications as in the oil and gas field, where some water data, such as temperature and pH, needs to be measured and collected from different regions [8], [9]. UVLC has major impediments such as turbidity that can lead to signal absorption and scattering. Hence, the UVLC communication range may decrease for less than 100 m, which motivates developing new techniques to support long ranges with high data rates [10]–[12].

Optical communication applications need detectors with fast response times; therefore, positive-intrinsic-negative (PIN) diodes and avalanche photon diodes (APDs) are widely used to meet the high-speed requirements. However, both PIN diodes and APDs are not suitable for less sensitive optical applications where the communication distance is large and/or the optical signal is weak. Single photon avalanche diode (SPAD) is designed to detect weak optical signal, where it operates with a higher reverse-bias voltage than the APDs. The operating voltage is well above the breakdown voltage to allow the operation in Geiger mode rather than the linear mode in APD permitting photons counting [13]–[16]. The high sensitivity characteristic of SPAD detectors was used to develop a reliable communication through long pipes in oil and gas industry without any ambient light in [15]. An accurate channel model based on two exponential terms was proposed in [17] to capture the long distance UVLC channel for SPAD based systems. The impact of turbulence was considered in signal space constellation design for multi-input-multi-ouput UVLC system that uses SPAD for detection in [18]. To this point and to the best of the authors' knowledge, there is no much effort paid to develop robust communication schemes for UVLC with SPAD detectors to mitigate the turbulence, moving obstacles and support high data rates for large distances.

In this paper, we propose using ARQ with finite transmission rounds in UVLC with SPAD receiver to support long range reliable communication against turbulence and moving obstacles. The proposed ARQ retransmission scheme aims to maintain acceptable quality of service (QoS) by targeting error free communication using one-bit feedback. Despite of the expected performance gain in terms of average error probability for the proposed ARQ-system, the energy consumption gradually increases with multiple trials to deliver the data correctly, especially, in poor quality channel. Therefore, we study the energy efficiency (EE) and throughput in addition to the average error probability to judge on the overall system performance from different perspectives. The contribution of our work is summarized as follows:

1) Analyze the average error probability of UVLC with SPAD detector assuming large scale fading model of two exponential terms that is suitable to long distance communications in addition to the impact of turbulence that is modeled as lognormal distribution and shot noise.
2) Propose using ARQ with finite number of transmissions for UVLC with SPAD detector and analyze the average error probability.
3) Analyze the throughput and average EE for a finite number of transmissions.
4) We numerically evaluate the average error probability, EE, and throughput and discuss the tightness of approximated analysis to numerical results.

The remainder of manuscript is organized as follows. First, we describe system for the ARQ technique in Section 2. In Sections 3, 4, and 5, we derive the analysis for PER, throughput, and

average EE for the proposed system, respectively. In Section 6, we present the numerical results that inspect the average throughput, EE, and PER for ARQ. Finally, we conclude the paper in Section 7.

2. System Description

In this section, we first describe the UVLC channel model, then we describe the received signal model in detail and finally discuss the ARQ scheme.

2.1 Channel Model

Underwater optical channel is subjected to different major impairments such as inherent energy loss and turbulence. The energy loss of transmitted optical signal is done by photons and other particles causing absorption and scattering, respectively. We use the two exponential power loss model for long distance underwater channel that is expressed as [17],

$$h(z) = A\,\exp(-Bz) + C\,\exp(-Dz). \tag{1}$$

where z represents the distance in meters and the parameters A, B, C and D are obtained by Monte Carlo numerical simulations [7], [17], [19].

The propagation of the optical signal can be also impeded by the turbulence that introduces sudden variations due to the change in refractive index. The main sources of such phenomena are temperature, salinity and the underwater air bubbles. The channel fading amplitude is modeled with lognormal distribution as

$$f_\alpha(\alpha) = \frac{1}{2\alpha\sqrt{2\pi\sigma_X^2}}\exp\left(-\frac{(\ln(\alpha) - 2\mu_X)^2}{8\sigma_X^2}\right), \tag{2}$$

where μ_X and σ_X^2 are the mean and the variance of the Gaussian distributed log-amplitude factor $X = 0.5\ln\alpha$. To normalize α such that $\mathbf{E}[\alpha] = 1$, we impose $\mu_X = -\sigma_X^2$ [18], [20]. Now we can mathematically express the joint channel impulse response $h_n(z)$ for our UVLC scenario as

$$h_n(z) = \alpha_n\, h(z). \tag{3}$$

where n is the retransmission index that corresponds to the n-th ARQ round.

2.2 Transmission Model

We assume a single UVLC link with a light emitting diode (LED) or a laser diode (LD) at the transmitter and a SPAD at the receiver side. For the pointing concern we assume that LED/LD is in the line of sight with the SPAD and the field of view of detector is wide enough to get the optical beam transmitted through source and provided symbol interference free link for under water optical communication. We use intensity modulation and direct detection (IM/DD) technique, because of its low cost and ease of implementation in UVLC systems. Orthogonal on-off keying is used as a transmitted signal in this work with off signal with LED transmitted power $P_s = 0$ and on with $P_s = 2P_0$, achieving average power $\bar{P}_s = P_0$. Each information packet consists of L symbols that are represented as $\mathbf{s} = [s(1), s(2), \cdots, s(L)]$ where ℓ is index to the symbol and $\ell = 1, 2, \cdots, L$. We assume that each channel is independent and identically distributed (iid) with lognormal mean $2\mu_X$ and variance $2\sigma_X^2$. Moreover we assume quasi static channel that employs each transmitted packet suffers from independent fading with coherent time longer than the packet duration. The received number of photons at the n-th transmission for the ℓ-th symbol at the SPAD detector is mathematically expressed as

$$r_n(\ell) = \zeta\alpha_n(\ell)s(\ell) + n_0, \tag{4}$$

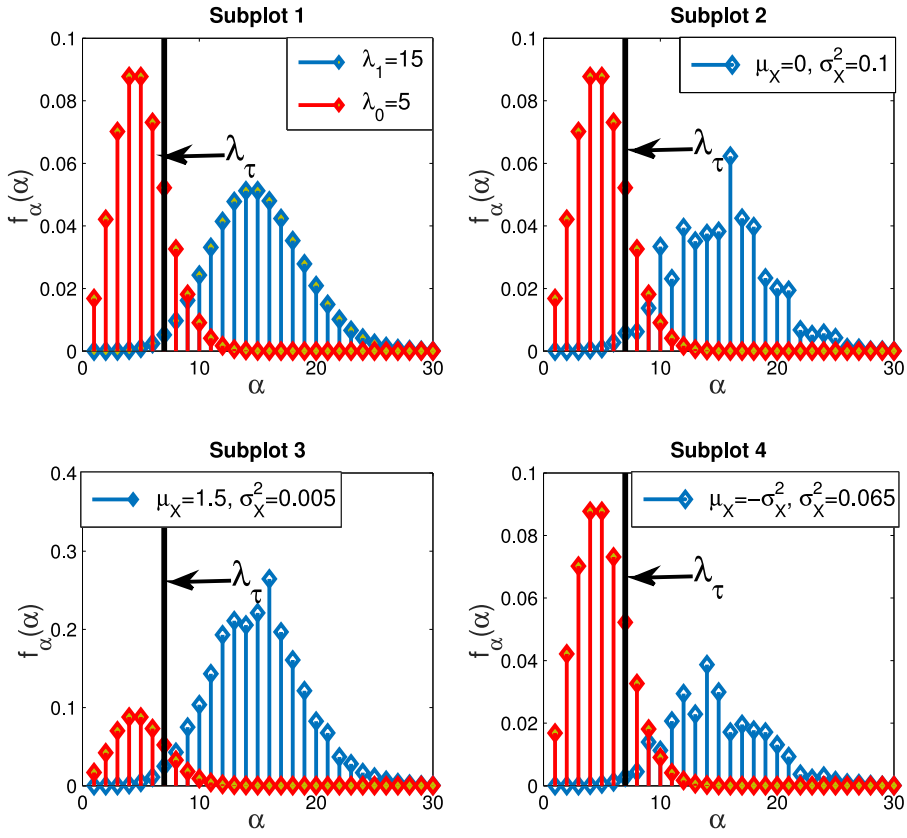

Fig. 1. log normal fading affect on data transmission through shot noise for different μ_X and σ_X^2.

where n_0 is the shot noise that represnts the random received number of photons in case of no-transmission, i.e., when $s(\ell) = 0$. To model the photon counting, Poisson statistics are adopted, with $n_0 \sim$ poisson(λ_0) where $\lambda_0 = N_{\text{DCR}} T_{\text{b}}$ is the average number of received photons when $s(\ell) = 0$ with N_{DCR} denotes the dark count ratio of the SPAD receiver in the presence of the shot noise and T_{b} represents the bit time duration [21]. On the other hand, when $s(\ell) = 1$, the average received number of photons is $\lambda_1 = E\alpha 2\zeta P_{\text{s}} + \lambda_0$, where $\zeta = T_{\text{b}} G_{\text{t}} \eta \eta_0 h_{\text{c}}$, $\eta = \frac{C_{\text{PDE}}}{E}$ where C_{PDE} is the photon detection efficiency, E is the energy of a photon in water, h_{c} is the well known Planks constant, η_0 is the gain of the optical system, which captures field-of-view angle of the SPAD and G_t is the intensity gain [17]. Throughout our study, we assume that transmitter and receiver planes are aligned to the light beam such that the receiver is able to effectively detect the light beam [17].

Fig. 1 shows the effect of different μ_X and σ_X^2 of the lognormal random variable on the original density function of received data. As a benchmark, the unfaded received signal distribution is depicted in Subplot 1 where λ_τ is denoting the threshold used to decide about the transmitted bit. The rest of Subplots show different faded scenarios for different values of μ_X and σ_X^2. It is clear that μ_X scales the density while σ_X^2 adds randomness to the original density as in subplot 2. Subplot 4 depicts the μ_X and σ_X^2 corresponding to weak turbulence scenario.

2.3 Automatic Repeat Request Scheme

We assume using ARQ scheme where the system requests packet retransmission if it is not decoded successfully according to the cyclic redundancy check (CRC). The threshold decision (λ_τ) of whether 0 or 1 is received is based on the received number of photons. We use the optical criteria in [17] to obtain the threshold, which comes actually from the number of received

photons at the SPAD detector. The transceiver continues to retransmit the packet until packet is received correctly or maximum transmission limit N is met. We use one bit feedback per packet and assume the existence of an acoustic feedback channel, which is typically available for underwater communication. Moreover, we assume limited transceivers capabilities that use uncoded signals, which lead to inferior performance to the ARQ systems with adaptive modulation and coding. In the following section, we analyze the error probability for ARQ system with a maximum of N transmissions.

3. Error Probability Analysis

In this section, we aim at evaluating the average packet error rate (PER) of the ARQ scheme for a maximum of N transmissions to deliver a data packet with L symbols which include 1 bit/symbol. To this end, we first express the average bit error rate (BER), then we develop the PER expression considering N ARQ transmission rounds.

Proposition 1: The BER of a SPAD receiver in UVLC link subjected to a lognormal turbulence is expressed as,

$$P_{\mathrm{e}} = \frac{1}{2}\left(1 - \sum_{r=0}^{\lambda_\tau} \frac{\lambda_0^r}{r!}\exp(-\lambda_0)\right) + \frac{1}{4\sqrt{2\pi\sigma_X^2}}\exp(-\lambda_0)\sum_{r=0}^{\lambda_\tau}\frac{\lambda_0^r}{r!}\sum_{j=0}^{r}\binom{r}{j}\kappa^r\sum_{i=1}^{N_{\mathrm{P}}} w_i y(X_i) \tag{5}$$

with $\kappa = \dfrac{\zeta 2P_{\mathrm{s}}}{\lambda_0}$ and $y(X_i)$ is expressed as

$$y(X_i) = \frac{X_i^{r-1}}{(2\zeta P_{\mathrm{s}})^r}\exp\left(-\frac{(\ln(\frac{X_i}{2\zeta P_{\mathrm{s}}}) - 2\mu_X)^2}{8\sigma_X^2}\right), \tag{6}$$

where X_i is the i-th zero of Laguerre polynomials and w_i is the corresponding weight defined as $w_i = \frac{X_i}{(N_{\mathrm{P}}+1)^2[L_{n+1}(X_i)]^2}$ [22, page 890][1].

Proof: The distribution of the received number of photons when $s(\ell) = 0$ and $s(\ell) = 1$ is expressed, respectively, as

$$\begin{aligned} p(r, \lambda_0) &= \frac{\lambda_0^r}{r!}\exp(-\lambda_0), \\ p(r, \lambda_1) &= \frac{\lambda_1^r}{r!}\exp(-\lambda_1). \end{aligned} \tag{7}$$

The BER for a given turbulence α is expressed as,

$$P_{\mathrm{e}/\alpha} = \frac{1}{2}\left(1 - \sum_{0}^{\lambda_\tau}\frac{\lambda_0^r}{r!}\exp(-\lambda_0) + \sum_{0}^{\lambda_\tau}\frac{\lambda_1^r}{r!}\exp(-\lambda_1)\right), \tag{8}$$

where the optimum detection threshold is expressed for a given α in [17] as $\lambda_\tau = \lceil \frac{\zeta 2P_{\mathrm{s}}E\alpha}{\ln\left(1+\frac{\zeta 2P_{\mathrm{s}}E\alpha}{\lambda_0}\right)} \rceil$. Then, we take the expectation of (8) over lognormal channel obtaining

$$P_{\mathrm{e}} = \frac{1}{2}\int_0^\infty \left[1 - \sum_{r=0}^{\lambda_\tau}\frac{\lambda_0^r}{r!}\exp(-\lambda_0) + \exp(-\lambda_1)\sum_{r=0}^{\lambda_\tau}\frac{\lambda_1^r}{r!}\right] f_\alpha(\alpha)d\alpha \tag{9}$$

The first two terms in above equation are independent of the lognormal distribution, so we need only to solve the third term, which is written as

$$I = \frac{1}{2}\exp(-\lambda_1)\int_0^\infty \sum_{r=0}^{\lambda_\tau}\frac{\lambda_1^r}{r!} f_\alpha(\alpha)d\alpha. \tag{10}$$

[1] See formula 25.4.45 and Table 25.9 for X_i and w_i.

Then, by simplifying (10) using binomial theorem, we get

$$I = \frac{1}{4\sqrt{2\pi\sigma_X^2}} \exp(-\lambda_0) \sum_{r=0}^{\lambda_\tau} \frac{\lambda_0^r}{r!} \sum_{j=0}^{r} \binom{r}{j} \kappa^r \int_0^\infty \exp(-\zeta\alpha 2P_s) \alpha^{r-1} \exp\left(-\frac{(\ln(\alpha) - 2\mu_X)^2}{8\sigma_X^2}\right) d\alpha. \quad (11)$$

To solve (11), we first change the variable as $\alpha = \frac{X}{\zeta 2P_s}$ obtaining

$$I = \frac{1}{4\sqrt{2\pi\sigma_X^2}} \exp(-\lambda_0) \sum_{r=0}^{\lambda_\tau} \frac{\lambda_0^r}{r!} \sum_{j=0}^{r} \binom{r}{j} \kappa^r \int_0^\infty \exp(-X) \frac{X^{r-1}}{(2\zeta P_s)^r} \exp\left(-\frac{(\ln(\frac{X}{2\zeta P_s}) - 2\mu_X)^2}{8\sigma_X^2}\right) dX, \quad (12)$$

then, we approximate the integral in (12) numerically by using Laguerre-Gauss Quadrature polynomial [22, page 890] and get the following approximation that depends on number of terms N_P,

$$I = \frac{1}{4\sqrt{2\pi\sigma_X^2}} \exp(-\lambda_0) \sum_{r=0}^{\lambda_\tau} \frac{\lambda_0^r}{r!} \sum_{j=0}^{r} \binom{r}{j} \kappa^r \sum_{i=1}^{N_P} w_i y(X_i), \quad (13)$$

where $y(X_i)$ and w_i where X_i is the i-th zero of Laguerre polynomials and w_i is the corresponding weight [22, page 890]. Now by substituting (13) in (9), we get (5) and prove Proposition 1.

Proposition 2: The packet error probability p_{ϵ_N} of UVLC system with a SPAD detector and ARQ scheme with a maximum of N transmissions and L bits per packet is expressed in (14).

$$p_{\epsilon_N} = \left[1 - \left(\frac{1}{2} - \frac{1}{2} \sum_{r=0}^{\lambda_\tau} \frac{\lambda_0^r}{r!} \exp(-\lambda_0) + \frac{1}{4\sqrt{2\pi\sigma_X^2}} \exp(-\lambda_0) \sum_{r=0}^{\lambda_\tau} \frac{\lambda_0^r}{r!} \sum_{j=0}^{r} \binom{r}{j} \kappa^r \sum_{i=1}^{N_P} w_i y(X_i)\right)^L\right]^N \quad (14)$$

Proof: Under the assumption of independent identically distributed (iid) lognormal fading channels, the probability of receiving an error-free packet of length L bits in each transmission is $p_c = (1 - P_e)^L$. Moreover, the probability of receiving a packet with errors after n transmissions is $p_{\epsilon_n} = (1 - p_c)^n$. Therefore, the PER after N transmissions is expressed as

$$p_{\epsilon_N} = (1 - p_c)^N = \left(1 - (1 - P_e)^L\right)^N. \quad (15)$$

Then, by using the results of Proposition 1 and (15), we get (14) and prove Proposition 2.

4. Throughput Analysis

ARQ schemes succeed to reduce error probability significantly by allowing packet retransmissions. However, increasing N may degrade the transmission rate of the UVLC with SPAD detector systems. Therefore, it is imperative to evaluate the performance of the proposed system based on the throughput, denoted as $\bar{\eta}(N)$, through the following proposition.

Proposition 3: The throughput $\bar{\eta}(N)$ achieved in UVLC with SPAD detector and ARQ with maximum N *transmission* attempts to deliver a packet of length L bits is expressed as,

$$\bar{\eta}(N) = \sum_{n=1}^{N} \frac{R}{n} (1 - p_{\epsilon_1}) \left(1 - (1 - P_e)^L\right)^{n-1}. \quad (16)$$

Proof: The average throughput of the ARQ retransmission scheme for N rounds of transmission is written as the average N discrete events as

$$\bar{\eta}(N) = \sum_{n=1}^{N} R_n f_n, \quad (17)$$

where R_n is the rate of each event that is given as $R_n = \frac{R}{n}$ and f_n is the corresponding event probability representing the error-free detection of the data packet after exactly the n-th transmission,

TABLE 1
Monte Carlo Numerical (MCS) Simulation Parameter for Oceanic Water

A	0.0519135
B	0.1592843
C	0.1189797
D	0.5071980

which is expressed as a function of the packet error rate as,

$$\begin{aligned} f_n &= (1 - p_{\epsilon_1}) P_{\epsilon_{n-1}}, \\ &= (1 - p_{\epsilon_1}) \left(1 - (1 - P_e)^L\right)^{n-1} \end{aligned} \tag{18}$$

Thus, by substituting (18) and R_n in (17), we obtain (16), which proves the Proposition 3.

5. Energy efficiency Analysis

Energy consumption is one of the important designing aspects in next generation wireless networks [23]. The proposed ARQ based system pays extra energy with each retransmission to reduce error probability. Therefore, we need to monitor the energy consumption of the proposed system, where providing substantial energy sources is not always manageable. As such, we analyze the average EE defined as the ratio between successfully received data in bits and the corresponding energy consumption in the following proposition.

Proposition 4: The average EE $\bar{\eta}_{\text{EE}}(N)$ required to deliver a packet of L bits successfully using a maximum of N transmission attempts in UVLC system with SPAD detector is expressed as,

$$\bar{\eta}_{\text{EE}}(N) = \sum_{n=1}^{N} \frac{R}{nP_{\text{s}}} (1 - p_{\epsilon_1}) \left(1 - (1 - P_e)^L\right)^{N-1} \tag{19}$$

where P_{s} represents the average power required for single transmission.

Proof: Similar to proof of proposition 3, one can follow similar steps to prove (19) for N ARQ transmission rounds with the average power transmitted in each transmission is P_{s}.

6. Simulation

In this section, we investigate the PER, throughput and EE performance of the proposed ARQ method for the proposed SPAD receiver system with log normal fading and underwater adsorption and scattering using analysis and monte Carlo simulations with respect to different system parameters. The parameters for channel impulse response due to absorption and scattering in coastal water are given in Table 1. In simulation setup, we consider packet size of length $L = 50$ bits transmitted over log normal fading channel. We assume that channel is quasi-static channel for one transmission round hence each channel realization is independent for each symbol in first and subsequent transmission round of ARQ in case of CRC failure. We use $N_{\text{P}} = 25$ point Laguerre-Gauss method to approximate the integral in (12). Throughout the following numerical results, unless otherwise specified, we assume the data is transmitted with rate $R = 1$ Kbits/sec and transmitted with average transmission power per symbol $P_{\text{s}} = 30$ dBm and $\alpha \sim \log \mathcal{N}(-\sigma_\chi^2, \sigma_\chi^2)$, where $\sigma_\chi^2 = 0.0625$. The constants meters used for SPAD and UW optics are also given in Table 2. The plotted results depict PER, the throughput, and EE for ARQ with N transmission versus different system parameters such as power, N and distance.

We provide comparison of analysis and simulation for PER versus different parameters and the results demonstrate that the analysis provides tight bound to the PER simulation, whereas,

TABLE 2
Parameters for SPAD and Optical Communication

parameter	values
(C_{PDE})	0.35
(N_{DCR})	50
T_b	100 msec
G_t	3.95
η_0	41.791044
η	9.353×10^{17}

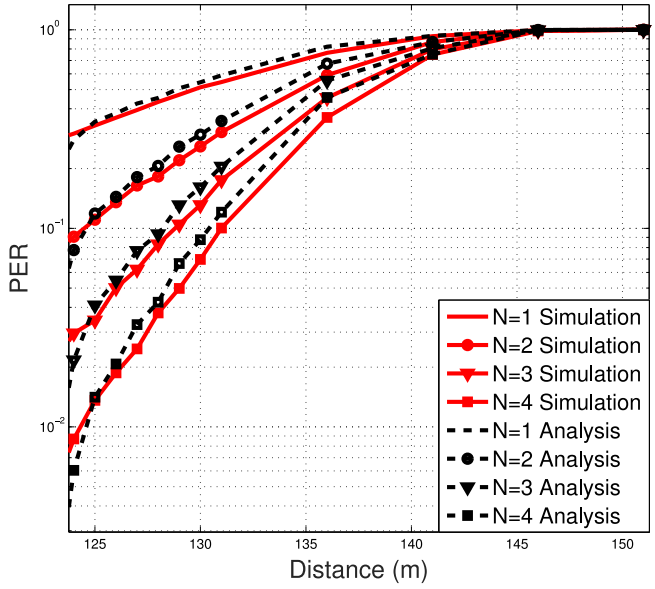

Fig. 2. Average PER performance comparison using analysis and simulation vs distance for $N = 1, 2, 3$ and 4 for $P_s = 30$ dBm.

we evaluate throughput and EE numerically using analysis knowing that EE and throughput are function of PER and analysis provides close bound on packet error. Moreover we use optimal threshold detection λ_τ for both simulation and analysis.

To this end, we first investigate the PER from simulations and PER analysis from (14) vs distance for different number of transmission rounds N in Fig. 2. The result shows that analysis is very close to simulation for $N = 1, 2, 3$ and 4 and this marginal gap between PER from analysis and simulation demonstrates the accuracy of PER analysis in (14) for optimal threshold on detection λ_τ. Moreover, its is clear from the Fig. 2 that underwater communication is highly sensitive to distance even using SPAD receivers, and PER decline with the increase in distance. Result also depicts that PER performance of ARQ round proliferates at smaller distance with increase in N, while as the distance increase the effect of N starts to diminish and all PER curves converge to single transmission that is, for $N = 1$ for larger distance after 145 m.

The Fig. 3 represents the PER with versus power for N ARQ rounds. The simulation and analysis result shows that by increasing power the PER decreases for $N = 1, \cdots, 4$. Furthermore the figure

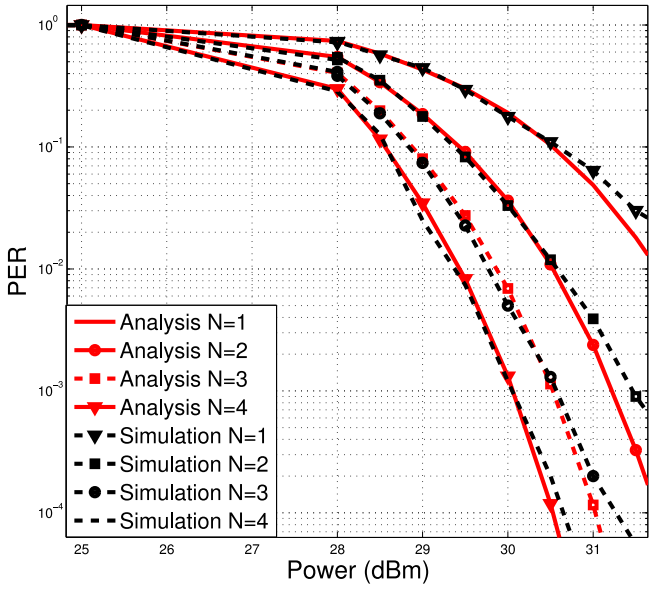

Fig. 3. Average PER performance comparison using analysis and simulation versus power P_s for $N = 1, 2, 3$ and 4 for distance $z = 130$.

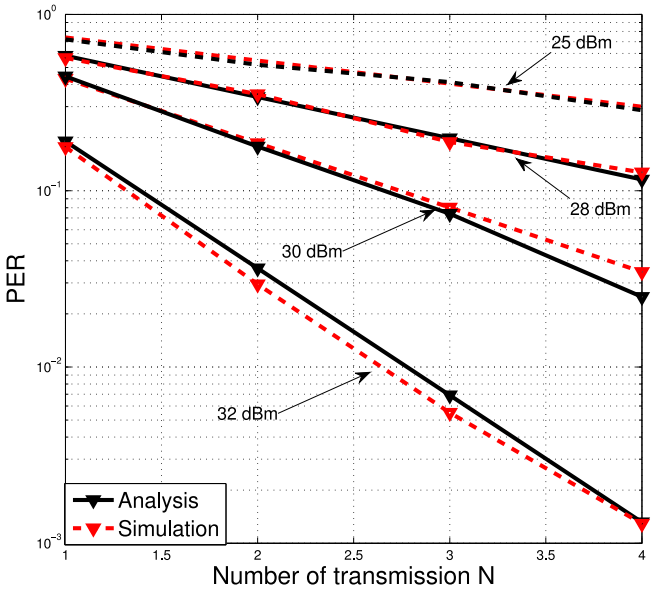

Fig. 4. Average PER performance comparison using analysis and simulation versus N for different P_s (dBm).

also elaborates the fact that at low power $P_s < 26$, N does not plays a significant role and for all N the PER converges to single transmission and similar to Fig. 2, PER simulation and PER analysis are marginally tight.

In this Fig. 4, PER comparison is plotted versus different N, depicts that increasing the number of ARQ rounds N increases the probability of error-free detection of packet for all P_s. Moreover, it also shows that analysis provides the tight bound on PER.

The Fig. 5 represents $\bar{\eta}_{EE}$ comparison with respect to distance for $N = 1, 2, 3, 4$ and 5. The numerical result suggests that $\bar{\eta}_{EE}$ decreases as the transceiver distance increases for all N. Note

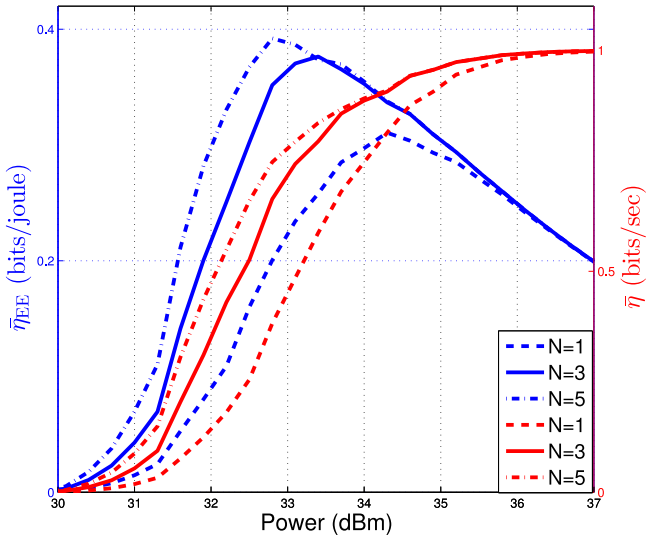

Fig. 5. Average EE for ARQ versus distance for different transmission rounds N.

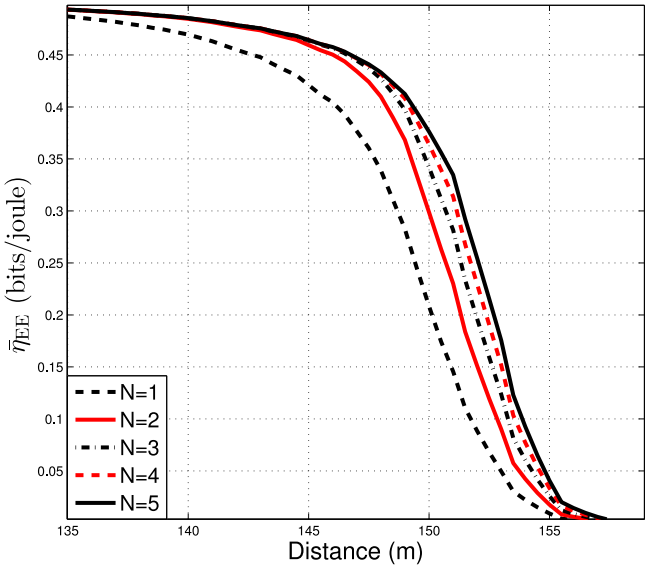

Fig. 6. Average EE for ARQ versus power P_{s} (dBm) with different N.

that $\bar{\eta}_{\mathrm{EE}}$ shows a considerable gain by increasing N but after as N increases to higher values the $\bar{\eta}_{\mathrm{EE}}$ starts to converge and this trend is observable because EE for $N = 4$ and $N = 5$ are very tight.

In Fig. 6, the trade-off relationship between EE and throughput is expressed versus different transmitted power and their comparison is provided. We observe the well-known relationship of EE versus the power P_{s}, that is increasing the power P_{s} improves the EE till the optimal EE point is reached after that EE starts to degrade by increases in P_{s}, showing the unnecessary power transmission. While throughput is directly proportional to the power. However using different transmission round helps to increase EE and throughput performance before the convergence is achieved for $P_{\mathrm{s}} > 36$ dBm. The values of the constants are given in Table 2.

7. Conclusion

In this paper, we derive the expression for packet error rate in presence of lognormal turbulence and shot noise. These performance analysis is proposed in such a way to study the effective parameters such as power, distance and number of transmission rounds to target error-free communication using SPAD to acquire longer communication range. We also obtain the results using monte Carlo simulations and provide the comparison of PER using simulations and analysis versus different parameter and results demonstrate the subtle gap that shows the effectiveness of analysis using 25-points Laguerre-Gauss Quadrature approach. Given that analysis provides tight bound to simulation, we also analyzed the effective throughput and EE for the truncated ARQ with N rounds and their trade-off.

References

[1] C. M. Gussen, P. S. Diniz, M. L. Campos, W. A. Martins, F. M. Costa, and J. N. Gois, "A survey of underwater wireless communication technologies," *J. Commun. Inf. Sys.*, vol. 31, no. 1, pp. 242–255, 2016.

[2] M. Gao, W.-S. Soh, and M. Tao, "A transmission scheme for continuous ARQ protocols over underwater acoustic channels," in *Proc. IEEE Int. Conf. Commun.*, 2009, pp. 1–5.

[3] M. A. Khalighi and M. Uysal, "Survey on free space optical communication: A communication theory perspective," *IEEE Commun. Surveys Tut.*, vol. 16, no. 4, pp. 2231–2258, Oct.–Dec. 2014.

[4] A. M. Abdelhady, O. Amin, A. Chaaban, and M.-S. Alouini, "Downlink resource allocation for multichannel TDMA visible light communications," in *Proc. IEEE Global Conf. Signal Inform. Process.*, Greater Washington, D.C., USA, 2016, pp. 1–5.

[5] P. H. Pathak, X. Feng, P. Hu, and P. Mohapatra, "Visible light communication, networking, and sensing: A survey, potential and challenges," *IEEE Commun. Surveys Tut.*, vol. 17, no. 4, pp. 2047–2077, Oct.–Dec. 2015.

[6] D. Wu, W.-D. Zhong, Z. Ghassemlooy, and C. Chen, "Short-range visible light ranging and detecting system using illumination light emitting diodes," *IET Optoelectron.*, vol. 10, no. 3, pp. 94–99, 2016.

[7] S. Tang, Y. Dong, and X. Zhang, "Impulse response modeling for underwater wireless optical communication links," *IEEE Trans. Commun.*, vol. 62, no. 1, pp. 226–234, Jan. 2014.

[8] H. Kaushal and G. Kaddoum, "Underwater optical wireless communication," *IEEE Access*, vol. 4, pp. 1518–1547, 2016.

[9] Z. Zeng, S. Fu, H. Zhang, Y. Dong, and J. Cheng, "A survey of underwater optical wireless communications," *IEEE Commun. Surveys Tut.*, vol. 19, no. 1, pp. 204–238, Jan.–Mar. 2017.

[10] E. Fisher, I. Underwood, and R. Henderson, "A reconfigurable single-photon-counting integrating receiver for optical communications," *IEEE J. Solid-State Circuits*, vol. 48, no. 7, pp. 1638–1650, Jul. 2013.

[11] T. J. Petzold, "Volume scattering functions for selected ocean waters," DTIC Document, Tech. Rep. No. SIO-REF-72-78, 1972.

[12] J. W. Giles and I. N. Bankman, "Underwater optical communications systems. part 2: basic design considerations," in *Proc. IEEE Military Commun. Conf.*, 2005, pp. 1700–1705.

[13] S. Gnecchi *et al.*, "Analysis of photon detection efficiency and dynamic range in SPAD-based visible light receivers," *J. Lightw. Technol.*, vol. 34, no. 11, pp. 2774–2781, Jun. 2016.

[14] E. Fisher, I. Underwood, and R. Henderson, "A reconfigurable 14-bit 60GPhoton/s single-photon receiver for visible light communications," in *Proc. Eur. Solid-State Circuits Conf.*, 2012, pp. 85–88.

[15] Y. Li, S. Videv, M. Abdallah, K. Qaraqe, M. Uysal, and H. Haas, "Single photon avalanche diode (SPAD) VLC system and application to downhole monitoring," in *Proc. IEEE Glob. Commun. Conf.*, 2014, pp. 2108–2113.

[16] J. Zhang, L.-H. Si-Ma, B.-Q. Wang, J.-K. Zhang, and Y.-Y. Zhang, "Low-complexity receivers and energy-efficient constellations for SPAD VLC systems," *IEEE Photon. Technol. Lett.*, vol. 28, no. 17, pp. 1799–1802, Sep. 2016.

[17] C. Wang, H.-Y. Yu, and Y.-J. Zhu, "A long distance underwater visible light communication system with single photon Avalanche diode," *IEEE J. Photon.*, vol. 8, no. 5, Oct. 2016, Art. no. 7906311.

[18] L.-H. Si-Ma *et al.*, "Hellinger-distance-optimal space constellations for SPAD underwater MIMO-OWC systems," *IEEE Commun. Lett.*, vol. 18, no. 8, pp. 765–768, Apr. 2017.

[19] F. Akhoundi, J. A. Salehi, and A. Tashakori, "Cellular underwater wireless optical CDMA network: Performance analysis and implementation concepts," *IEEE Trans. Commun.*, vol. 63, no. 3, pp. 882–891, Mar. 2015.

[20] M. V. Jamali, F. Akhoundi, and J. A. Salehi, "Performance characterization of relay-assisted wireless optical CDMA networks in turbulent underwater channel," *IEEE Trans. Wireless Commun.*, vol. 15, no. 6, pp. 4104–4116, Jun. 2016.

[21] T. Mao, Z. Wang, and Q. Wang, "Receiver design for SPAD-based VLC systems under Poisson–Gaussian mixed noise model," *Opt. Exp.*, vol. 25, no. 2, pp. 799–809, Jan. 2017.

[22] M. Abramowitz and I. A. Stegun, *Handbook of Mathematical Functions: With Formulas, Graphs, and Mathematical Tables*. North Chelmsford, MA, USA: Courier Corporation, 1964, vol. 55.

[23] O. Amin, S. Bavarian, and L. Lampe, "Cooperative techniques for energy-efficient wireless communications," in *Green Radio Communication Networks*. Cambridge, U.K.: Cambridge Univ. Press, 2012, pp. 125–149.